Loss of circadian rhythmicity in aging *mPer1*$^{-/-}$ *mCry2*$^{-/-}$ mutant mice

Henrik Oster,[1] Stéphanie Baeriswyl,[1] Gijsbertus T.J. van der Horst,[2] and Urs Albrecht[1,3]

[1]Department of Medicine, Division of Biochemistry, University of Fribourg, 1700 Fribourg, Switzerland; [2]Department of Cell Biology & Genetics, Erasmus Medical Centre Rotterdam, 3000 DR Rotterdam, The Netherlands

The *mPer1*, *mPer2*, *mCry1*, and *mCry2* genes play a central role in the molecular mechanism driving the central pacemaker of the mammalian circadian clock, located in the suprachiasmatic nuclei (SCN) of the hypothalamus. In vitro studies suggest a close interaction of all mPER and mCRY proteins. We investigated mPER and mCRY interactions in vivo by generating different combinations of *mPer*/*mCry* double-mutant mice. We previously showed that *mCry2* acts as a nonallelic suppressor of *mPer2* in the core clock mechanism. Here, we focus on the circadian phenotypes of *mPer1*/*mCry* double-mutant animals and find a decay of the clock with age in *mPer1*$^{-/-}$ *mCry2*$^{-/-}$ mice at the behavioral and the molecular levels. Our findings indicate that complexes consisting of different combinations of mPER and mCRY proteins are not redundant in vivo and have different potentials in transcriptional regulation in the system of autoregulatory feedback loops driving the circadian clock.

[*Keywords*: Circadian clock; Per; Cry; aging; transcription]

Supplemental material is available at http://www.genesdev.org.

Received November 28, 2002; revised version accepted April 10, 2003.

The earth's rotation around the Sun has strongly influenced temporal organization of the mammalian organism manifested by near-24-h rhythms of biological processes (Pittendrigh 1993), including the sleep–wake cycle, energy metabolism, body temperature, renal activity, and blood pressure. These rhythms are maintained even in the absence of external time signals (*Zeitgeber*). They are driven by a central clock located in the suprachiasmatic nuclei (SCN) of the ventral hypothalamus (Rusak and Zucker 1979; Ralph et al. 1990). Because the internal period length generated by this pacemaker is not exactly 24 h, the clock has to be reset every day by an input pathway synchronizing the organism's biological processes with geophysical time. The daily variation in light intensity is monitored by photoreceptors in the eye that project into the SCN via the retinohypothalamic tract (RHT; Rusak and Zucker 1979) and the intergeniculate leaflet (IGL; Jacob et al. 1999). The oscillations generated in the SCN are translated into overt rhythms in behavior and physiology through output pathways that probably involve both chemical and electrical signals.

At the molecular level, circadian rhythms are generated by the integration of autoregulatory transcriptional/translational feedback loops (TTLs; Allada et al. 2001; Albrecht 2002; Reppert and Weaver 2002). In the mammalian system, the TTL can be subdivided into a positive and a negative limb. The positive limb is constituted by the PAS helix–loop–helix transcription factors CLOCK and BMAL1 that upon heterodimerization bind to "E-box" enhancer elements regulating transcription of *Period* (*mPer*) and probably also *Cryptochrome* (*mCry*) genes. The mPER and mCRY proteins are components of the negative limb that attenuate the CLOCK/BMAL1-mediated activation of their own genes and hence generate a negative feedback. A number of posttranslational events such as phosphorylation, ubiquitylation, degradation, and intracellular transport seem to be critical for the generation of oscillations in clock gene products and the stabilization of a 24-h period (Kume et al. 1999; Yagita et al. 2000, 2002; Lee et al. 2001; Miyazaki et al. 2001; Vielhaber et al. 2001; Yu et al. 2002). Additionally, the two limbs of the TTL are linked by the nuclear orphan receptor REV-ERBα, which is under the influence of *mPer* and *mCry* genes and controls transcription of *Bmal1* (Preitner et al. 2002). In mammals, three *Per* genes—*mPer1* (Sun et al. 1997; Tei et al. 1997), *mPer2* (Albrecht et al. 1997; Shearman et al. 1997), and *mPer3* (Zylka et al. 1998)—and two *Cry* genes—*mCry1* and *mCry2* (Miyamoto and Sancar 1998)—have been identified. Although *mPer3* seems not to be necessary for the generation of circadian rhythmicity (Shearman et al. 2000), *mPer1*, *mPer2*, and both *mCry* genes have been demonstrated to play essential roles in the central oscillator as well as in the light-driven input pathway to the clock (van der Horst et al. 1999; Vitaterna et al. 1999;

[3]Corresponding author.
E-MAIL urs.albrecht@unifr.ch; FAX 41-26-300-9735.
Article and publication are at http://www.genesdev.org/cgi/doi/10.1101/gad.256103.

Zheng et al. 1999, 2001; Albrecht et al. 2001; Bae et al. 2001; Cermakian et al. 2001). In addition to the master clock in the SCN, most cells of peripheral tissues possess a circadian oscillator with a molecular organization very similar to that of SCN neurons, but lacking light-responsiveness (Balsalobre et al. 1998; Yamazaki et al. 2000; Yagita et al. 2001).

The molecular mechanism of clock autoregulation has largely been studied in vitro (Gekakis et al. 1998; Kume et al. 1999; Miyazaki et al. 2001; Vielhaber et al. 2001; Yagita et al. 2000, 2002; Yu et al. 2002). These studies point to multiple physical interactions between all mPER and mCRY proteins. However, the time course of protein availability, modification, and localization is difficult to resolve in cell and slice cultures (Jagota et al. 2000; Hamada et al. 2001; Lee et al. 2001). To elucidate the functional relationship between the *mPer* and *mCry* genes in vivo, we started to inactivate different combinations of *mPer* and *mCry* genes in mice (Oster et al. 2002).

Here we show that *mPer1*$^{-/-}$ *mCry1*$^{-/-}$ mice maintain a functional circadian clock and that *mPer1*$^{-/-}$ *mCry2*$^{-/-}$ mice lose circadian rhythmic behavior after a few months. This loss of rhythmicity is accompanied by altered regulation of expression of core clock components and the clock output gene arginine vasopressin (AVP). Our results indicate that the amount of mPER and mCRY proteins and hence the composition of mPER/mCRY complexes are critical for generation and maintenance of circadian rhythms.

Results

Generation of mPer1$^{-/-}$ mCry1$^{-/-}$ *and* mPer1$^{-/-}$ mCry2$^{-/-}$ *mice*

To begin to understand the in vivo function of the *mPer* and *mCry* genes in the clock mechanism, we generated mice with disruptions in both the *mPer1*/*mCry1* or *mPer1*/*mCry2* genes. Mice with a deletion of the *mPer1* gene (Zheng et al. 2001) were crossed with *mCry1*$^{-/-}$ or *mCry2*$^{-/-}$ mice, respectively (van der Horst et al. 1999). The double-heterozygous offspring were intercrossed to produce wild-type and homozygous mutant animals. *mPer1*$^{-/-}$ *mCry1*$^{-/-}$ and *mPer1*$^{-/-}$ *mCry2*$^{-/-}$ mice (representative genotyping shown in Fig. 1A) were obtained at the expected Mendelian ratios and were morphologically indistinguishable from wild-type animals. The animals appeared normal in fertility, although in *mPer1*/*mCry* double-mutant mice, the intervals between two litters seem to increase significantly with progressing age (data not shown).

mPer1 *acts as a nonallelic suppressor of* mCry1

To determine the influence of inactivation of the *mCry1* gene on circadian behavior of *mPer1*$^{-/-}$ mice, mutant and wild-type animals were individually housed in circadian activity-monitoring chambers (Albrecht and Oster 2001; Albrecht and Foster 2002) for analysis of wheel-running activity. Mice were kept in a 12-h light/12-h dark cycle (LD 12:12, or LD) for several days to establish entrainment, and were subsequently kept in constant darkness (DD). Under LD and DD conditions, *mPer1*$^{-/-}$ *mCry1*$^{-/-}$ animals displayed activity and clock gene expression patterns similar to that of wild-type mice (Fig. 1B,C; Supplementary Fig. 1). Under DD conditions, *mPer1*$^{-/-}$ *mCry1*$^{-/-}$ mutant mice displayed a period length (τ) of 23.7 ± 0.2 h (mean ± S.D., n = 15), which is similar to that of wild-type animals (τ = 23.8 ± 0.1 h; n = 17). Thus, an additional deletion of *mPer1* rescues the short-period phenotype of *mCry1*-deficient mice (van der Horst et al. 1999), indicating that *mPer1* acts as a nonallelic suppressor of *mCry1*.

Loss of circadian wheel running activity rhythms in aging mPer1$^{-/-}$ mCry2$^{-/-}$ *double-mutant mice*

Analysis of circadian behavior of *mPer1*$^{-/-}$ *mCry2*$^{-/-}$ animals under LD conditions revealed that in young *mPer1*$^{-/-}$ *mCry2*$^{-/-}$ animals (between 2 and 6 mo old), the onset of activity was delayed as compared with wild-type animals and the highest activity could be observed in the second half of the night, with masking of activity during the first hours of the day (Fig. 1D). Under DD conditions, these animals display rhythmic behavior with a long period (τ) of 25.3 ± 0.2 h (mean ± S.D., n = 14) compared with wild-type animals (τ = 23.8 ± 0.1 h; n = 17; Fig. 1D,E).

Interestingly, *mPer1*$^{-/-}$ *mCry2*$^{-/-}$ animals that were >6 mo old displayed a markedly disturbed diurnal activity pattern under LD conditions (Fig. 1F), as evident from the very faint 24-h rhythm detected by χ^2 periodogram analysis (Fig. 1G). Under DD conditions, old *mPer1*$^{-/-}$ *mCry2*$^{-/-}$ mice were completely arrhythmic (Fig. 1F,I), which sharply contrasts the robust rhythmicity of young *mPer1*$^{-/-}$ *mCry2*$^{-/-}$ mice under similar conditions. The transition from a rhythmic to an arrhythmic phenotype in *mPer1*$^{-/-}$ *mCry2*$^{-/-}$ mice correlated well with age (Fig. 1H). Whereas all *mPer1*$^{-/-}$ *mCry2*$^{-/-}$ mice at an age between 2 and 6 mo display circadian activity patterns, 40% of animals between 6 and 12 mo of age have lost circadian rhythmicity. When animals reached the age of 1 yr or older, even 87% of the *mPer1*$^{-/-}$ *mCry2*$^{-/-}$ mice have become arrhythmic. We did not observe a comparable age-related loss of rhythmicity in wild-type, *mPer1*$^{-/-}$ and *mCry2*$^{-/-}$ mice (Fig. 1 H; Supplementary Fig. 2A–C) and not in *mPer1*$^{-/-}$ *mCry1*$^{-/-}$, *mPer2*^{Brdm1} *mCry1*$^{-/-}$ and *mPer2*^{Brdm1} *mCry2*$^{-/-}$ mice, respectively (Supplementary Fig. 2D).

Alterations in expression levels of clock components and the clock output gene Avp *in aging* mPer1$^{-/-}$ mCry2$^{-/-}$ *double-mutant mice*

To extend our observations to the molecular level, we examined the expression patterns of the *mPer2*, *mCry1*, and *Bmal1* genes in 6–12-month-old *mPer1*$^{-/-}$ *mCry2*$^{-/-}$

mice under LD and DD conditions. For simplicity, we will refer to "young" and "old" *mPer1*$^{-/-}$ *mCry2*$^{-/-}$ animals on the basis of rhythmic or arrhythmic behavior, respectively.

mPer2 mRNA expression in the SCN of young *mPer1*$^{-/-}$ *mCry2*$^{-/-}$ mice was comparable to that of wild-type animals under both LD and DD conditions with peak levels at *Zeitgeber* time (ZT) and circadian time (CT) 12, respectively (Fig. 2A,B). Interestingly, rhythmic *mPer2* mRNA expression was severely blunted in the SCN of old *mPer1*$^{-/-}$ *mCry2*$^{-/-}$ mice (Fig. 2A). As *mPer2* expression in old (6–12 mo) *mPer1*$^{-/-}$ and *mCry2*$^{-/-}$ single-mutant mice did not show a detectable reduction in amplitude under LD and DD conditions (Supplementary Fig. 3A,B), we conclude that the age-related loss of *mPer2* mRNA oscillation in *mPer1*$^{-/-}$ *mCry2*$^{-/-}$ animals is characteristic for the double-knockout status. Analysis of the peripheral circadian oscillator in the kidney revealed a normal *mPer2* mRNA expression profile in young *mPer1*$^{-/-}$ *mCry2*$^{-/-}$ mice kept under LD conditions, with maximal expression observed around ZT12 (Fig. 2D,E). In line with the data observed for the SCN, cyclic *mPer2* mRNA expression in the kidney is blunted in old *mPer1*$^{-/-}$ *mCry2*$^{-/-}$ mice (Fig. 2D,E). In conclusion, circadian oscillators lacking both *mPer1* and *mCry2* appear sensitive to aging.

To correlate mRNA expression to protein levels, we examined the presence of mPER2 protein in the SCN by immunohistochemistry. In wild-type and young *mPer1*$^{-/-}$ *mCry2*$^{-/-}$ mice, protein levels are high between ZT12 and ZT18 (Fig. 2C; Field et al. 2000), which is a few hours later than mRNA expression (Fig. 2A). In old *mPer1*$^{-/-}$ *mCry2*$^{-/-}$ mice, however, protein levels are low comparable to mRNA expression (Fig. 2A,C).

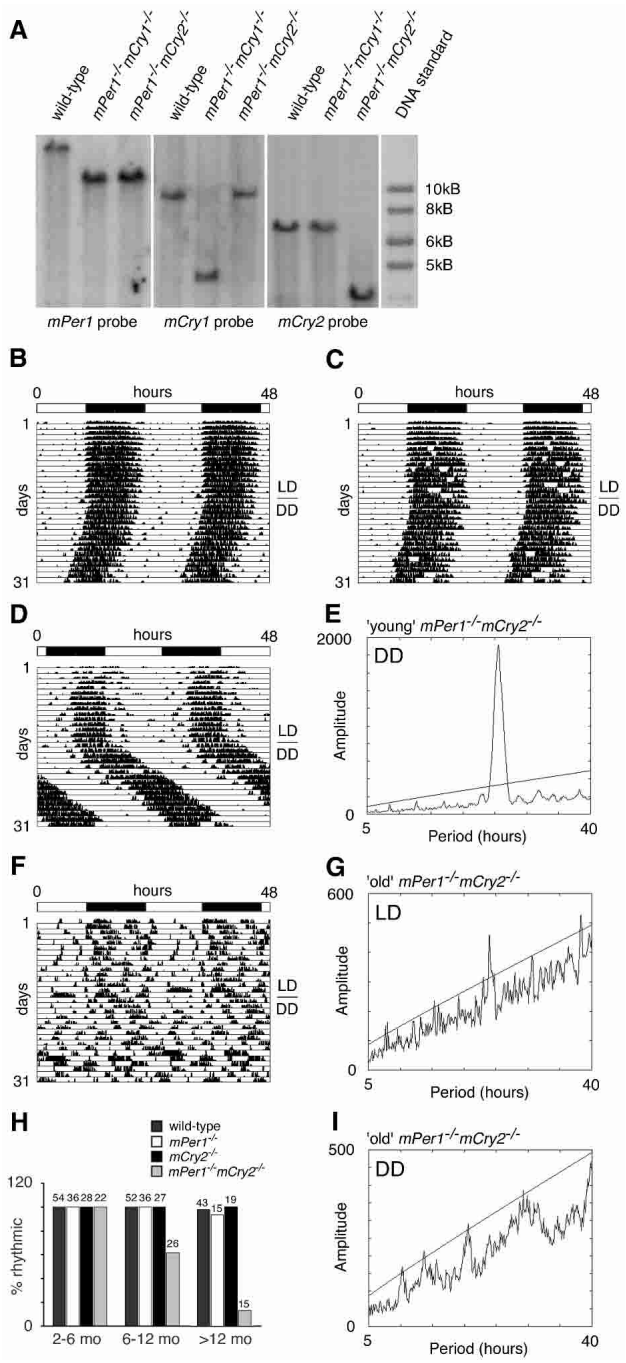

Figure 1. Generation of *mPer1mCry* double-mutant mice and representative locomotor activity records. (*A*) Southern blot analysis of wild-type, *mPer1*$^{-/-}$ *mCry1*$^{-/-}$, and *mPer1*$^{-/-}$ *mCry2*$^{-/-}$ tail DNA. The *mPer1* probe hybridizes to a 20-kb wild-type and a 11.8-kb mutant fragment of *Eco*RI-digested genomic DNA. The *mCry1* probe detects a 9-kb wild-type and a 4-kb *Nco*I-digested fragment of the targeted locus. In *mCry2* mutants, the wild-type allele is detected by hybridization of the probe to a 7-kb *Eco*RI fragment, whereas the mutant allele yields a 3.5-kb fragment. (*B–D,F*) Representative locomotor activity records of wild-type (*B*), *mPer1*$^{-/-}$ *mCry1*$^{-/-}$ (*C*), young *mPer1*$^{-/-}$ *mCry2*$^{-/-}$ (*D*), and old *mPer1*$^{-/-}$ *mCry2*$^{-/-}$ (*F*) animals kept in a 12-h light/12-h dark (LD) cycle and in constant darkness (DD; transition indicated by the horizontal line). Activity is represented by black bars and is double-plotted with the activity of the following light/dark cycle plotted to the *right* and below the previous light/dark cycle. The *top* bar indicates light and dark phases in LD. For the first 5 d in DD, wheel rotations per day were 20,000 ± 2500 (n = 17) for wild-type animals, 21,500 ± 7300 (n = 15) for *mPer1*$^{-/-}$ *mCry1*$^{-/-}$ mutants, 25,100 ± 6200 (n = 14) for young *mPer1*$^{-/-}$ *mCry2*$^{-/-}$ mutants, and 17,200 + 7900 (n = 9) for old *mPer1*$^{-/-}$ *mCry2*$^{-/-}$ mutants. (*E,G,I*) Periodogram analysis of young *mPer1*$^{-/-}$ *mCry2*$^{-/-}$ animals in DD (*E* corresponds to activity plot in *D*), and old *mPer1*$^{-/-}$ *mCry2*$^{-/-}$ animals in LD (*G* corresponds to activity plot in *F*) and DD (*I* corresponds to activity plot in *F*). Analysis was performed on 10 consecutive days in LD or DD after animals were allowed to adapt 5 d to the new light regimen. The ascending straight line in the periodograms represents a statistical significance of $p < 0.001$ as determined by the ClockLab program. (*H*) Age dependence of rhythmicity in wild-type (dark gray bar), *mPer1*$^{-/-}$ (white bar), *mCry2*$^{-/-}$ (black bar), and *mPer1*$^{-/-}$ *mCry2*$^{-/-}$ (light gray bar) mice. The animals tested were divided into three groups according to their age (2–6 mo, 6–12mo, and >12 mo old). Rhythmicity in DD was determined by periodogram analysis. The values on *top* of each bar indicate the total numbers of animals tested per group and genotype.

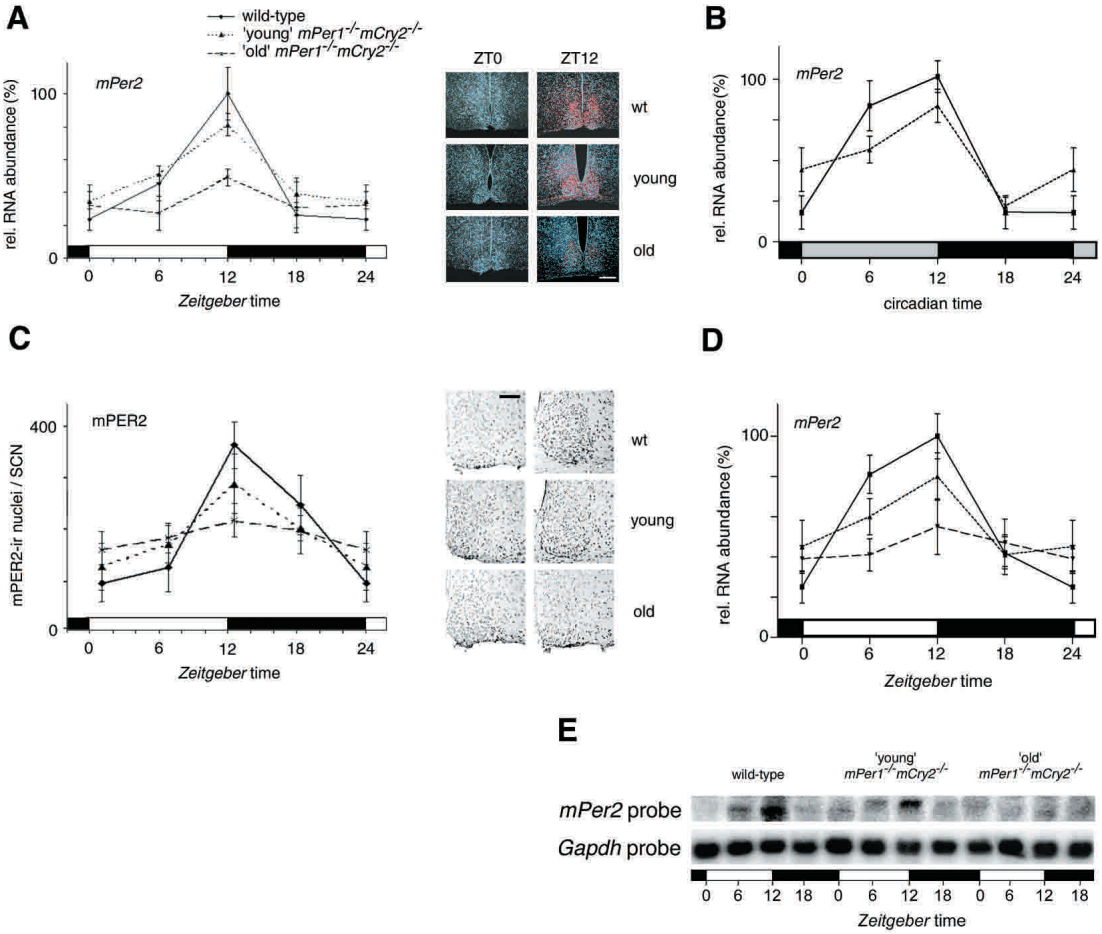

Figure 2. *mPer2* mRNA and mPER2 protein expression profiles of young and old *mPer1*$^{-/-}$ *mCry2*$^{-/-}$ mice. (*A*) Diurnal expression of *mPer2* in the SCN of wild-type (solid line), young *mPer1*$^{-/-}$ *mCry2*$^{-/-}$ (dotted line), and old *mPer1*$^{-/-}$ *mCry2*$^{-/-}$ (dashed line) mice in LD. In old double mutants, *mPer2* cycling is significantly dampened ($p < 0.05$). The black and white bars on the *X*-axis indicate the dark and light phases, respectively. All data presented are mean ± S.D. for three different experiments. (*Right* panels) Representative micrographs of SCN probed with an *mPer2* antisense probe at time points of minimal (ZT0) and maximal (ZT12) expression. Tissue was visualized by Hoechst dye nuclear staining (blue); silver grains are artificially colored (red) for clarification. Bar, 200 µm. (*B*) Circadian expression of *mPer2* in the SCN of wild-type (solid line) and young *mPer1*$^{-/-}$ *mCry2*$^{-/-}$ (dotted line) mice on the fourth day in DD. Gray and black bars on the *X*-axis indicate subjective day and night, respectively. (*C*) Diurnal variation of mPER2 immunoreactivity in the SCN of wild-type (solid line), young *mPer1*$^{-/-}$ *mCry2*$^{-/-}$ (dotted line), and old *mPer1*$^{-/-}$ *mCry2*$^{-/-}$ (dashed line) mice in LD. Quantification was performed by counting immunoreactive nuclei in the area of the SCN. In old double mutants, oscillation of mPER2 immunoreactivity is significantly dampened ($p < 0.05$) with medium numbers of immunoreactive nuclei. (*Right* panels) Representative micrographs of immunostained SCN at time points of minimal (ZT0) and maximal (ZT12) immunoreactivity. Bar, 100 µm. (*D*) Quantified Northern analysis of diurnal expression of *mPer2* in the kidney of wild-type (solid line), young *mPer1*$^{-/-}$ *mCry2*$^{-/-}$ (dotted line), and old *mPer1*$^{-/-}$ *mCry2*$^{-/-}$ (dashed line) mice in LD. (*E*) Representative Northern blot from kidney tissue from wild-type (*left*), young *mPer1*$^{-/-}$ *mCry2*$^{-/-}$ (*middle*), and old *mPer1*$^{-/-}$ *mCry2*$^{-/-}$ (*right*) mice sequentially hybridized with *mPer2* (*top* row) and *Gapdh* (*bottom* row) antisense probes. The black and white bars below the blots indicate dark and light phase, respectively.

mPER1/2 and mCRY1/2 proteins inhibit CLOCK/BMAL1-mediated transcriptional activation (Kume et al. 1999; Lee et al. 2001). Therefore, we investigated the expression pattern of *mCry1* in the SCN in *mPer1*$^{-/-}$ *mCry2*$^{-/-}$ mice. *mCry1* mRNA expression profiles peak at ZT12 and CT12 under LD and DD conditions, respectively (Fig. 3A,B; Okamura et al. 1999). Similar expression patterns were observed in *mPer1*$^{-/-}$, *mCry2*$^{-/-}$, and young *mPer1*$^{-/-}$ *mCry2*$^{-/-}$ mice (Fig. 3A,B; Supplementary Fig. 3C,D). Interestingly, *mCry1* mRNA levels displayed normal cycling in old *mPer1*$^{-/-}$ *mCry2*$^{-/-}$ mice in LD (Fig. 3A), which is in marked contrast to the blunted *mPer2* mRNA expression profile in these mice (Fig. 2A,B). We thus examined mCRY1 protein levels in the SCN by immunohistochemistry. In wild-type animals, mCRY1 protein levels are oscillating with peak expression between ZT12 and ZT18 (Fig. 3C), as reported previously (Field et al. 2000). Similarly, young *mPer1*$^{-/-}$ *mCry2*$^{-/-}$ mice displayed cycling expression of mCRY1 protein, but the trough mCRY1 protein levels (at ZT24) were higher than in wild-type animals (Fig. 3C). Strikingly, expression of mCRY1

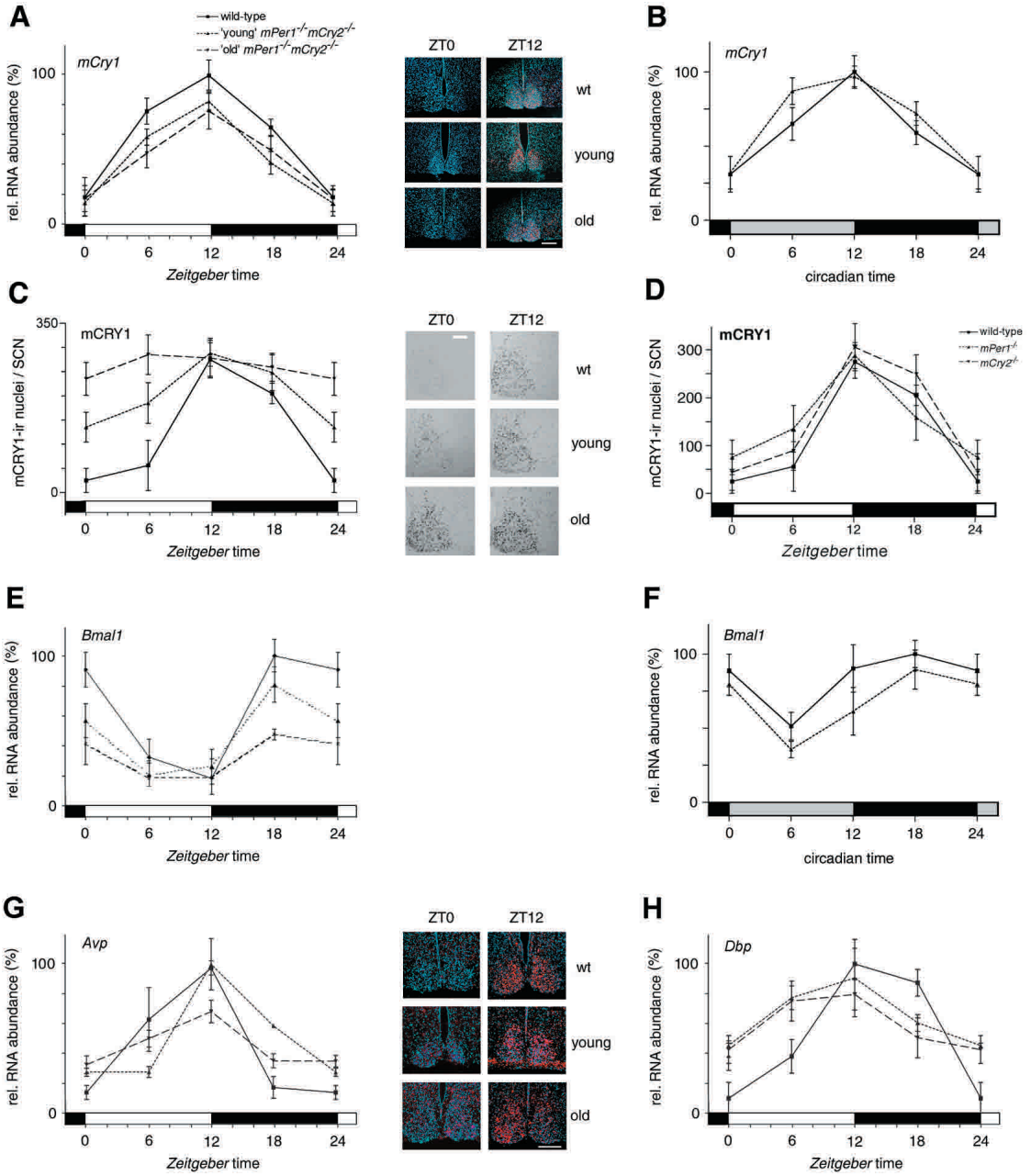

Figure 3. *mCry1* and *Bmal1* mRNA, and mCRY1 protein expression profiles of wild-type (solid line), young *mPer1*$^{-/-}$ *mCry2*$^{-/-}$ (dotted line), and old *mPer1*$^{-/-}$ *mCry2*$^{-/-}$ (dashed line) mice. (*A*) Diurnal expression of *mCry1* in the SCN in LD. The black and white bars on the *X*-axis indicate dark and light phases, respectively. (*Right* panels) Representative micrographs of SCN probed with the *mCry1* antisense probe at time points of minimal (ZT0) and maximal (ZT12) expression. Bar, 200 µm. (*B*) Circadian expression of *mCry1* in the SCN on the fourth day in DD. The gray and black bars on the *X*-axis indicate subjective day and night, respectively. (*C*) Diurnal variation of mCRY1 immunoreactivity in the SCN in LD. Quantification was performed by counting immunoreactive nuclei in the area of the SCN. In old double mutants, oscillation of mCRY1 immunoreactivity is significantly dampened ($p < 0.05$), with constantly high numbers of immunoreactive nuclei throughout the LD cycle. (*Right* panels) Representative micrographs of immunostained SCN at time points of minimal (ZT0) and maximal (ZT12) immunoreactivity. Bar, 100 µm. (*D*) Diurnal expression of mCRY1 protein in the SCN of wild-type (solid line), *mPer1*$^{-/-}$ (dotted line), and *mCry2*$^{-/-}$ (hatched line) mice. (*E*) Diurnal variation of *Bmal1* mRNA expression in the SCN in LD. In old double mutants, *Bmal1* cycling is significantly dampened ($p < 0.05$). (*F*) Circadian expression of *Bmal1* mRNA in the SCN on the fourth day in DD. (*G*) Diurnal time course of *Avp* mRNA expression in the SCN in LD. (*H*) Diurnal time course of *Dbp* mRNA expression in the SCN in LD. Tissue was visualized by Hoechst dye nuclear staining (blue); silver grains are artificially colored (red) for clarification. All data presented are mean ± S.D. for three different experiments.

protein became totally blunted in old *mPer1*$^{-/-}$ *mCry2*$^{-/-}$ mice, leading to almost constant high levels of mCRY1 protein throughout the 24-h LD cycle (Fig. 3C). Note that age-matched *mPer1*$^{-/-}$ and *mCry2*$^{-/-}$ single-

mutant mice display normal mCRY1 protein cycling (Fig. 3D).

We looked at *Bmal1* mRNA expression, a clock component of the positive limb, under LD and DD conditions. In wild-type and *mPer1*$^{-/-}$ animals, a maximum was seen at ZT and CT 18 in the SCN (Supplementary Fig. 3E,F) as previously observed (Honma et al. 1998). In *mCry2*$^{-/-}$ animals, the maximum of *Bmal1* expression was slightly delayed (Supplementary Fig. 3E,F). Young *mPer1*$^{-/-}$ *mCry2*$^{-/-}$ animals displayed a wild-type expression pattern, although the peak levels tended to be slightly decreased (Fig. 3E,F). In old *mPer1*$^{-/-}$ *mCry2*$^{-/-}$ mice, *Bmal1* mRNA levels were significantly blunted (Fig. 3E).

Because expression of core clock components is altered in old *mPer1*$^{-/-}$ *mCry2*$^{-/-}$ animals, we investigated whether this translates into a change in expression of output genes. *Arginine-vasopressin* (*Avp*) expression is significantly reduced in old *mPer1*$^{-/-}$ *mCry2*$^{-/-}$ animals (Fig. 3G), indicating physiological consequences linked to the aging process. *mPer1* and *mCry2* mutant mice do not exhibit this change in *Avp* expression (Albrecht and Oster 2001; Supplementary Fig. 3G). *Dbp* expression appeared also to be affected (Fig. 3H); however, this change is caused by the *Cry2* inactivation (Supplementary Fig. 3H) and is not specific to the *Per1 Cry2* double mutation.

Loss of light inducibility of mPer2 *mRNA and effect on delaying the clock phase in* mPer1$^{-/-}$ mCry2$^{-/-}$ *mice*

mPer expression can also be induced by phase-resetting light stimuli via the CREB signaling pathway (Motzkus et al. 2000; Travnickova-Bendova et al. 2002). To investigate whether aging affects light inducibility of the *mPer2* gene in the SCN of *mPer1*$^{-/-}$ *mCry2*$^{-/-}$ mice, we exposed young and old animals to a 15-min nocturnal light pulse at ZT14. Interestingly, induction of *mPer2* mRNA was significantly impaired in young *mPer1*$^{-/-}$ *mCry2*$^{-/-}$ mice when compared with wild-type animals ($p < 0.05$; Fig. 4A,B). This defect was even more pronounced in old *mPer1*$^{-/-}$ *mCry2*$^{-/-}$ mice ($p < 0.001$; Fig. 4A,B), indicating that the light signal transduction pathway might be affected. Therefore we set out to investigate light-dependent phosphorylation of CREB at position 133 (CREB-Ser^{133}). We found that in wild-type animals, phosphorylation at CREB-Ser^{133} was induced by light (Fig. 4C,D) as described previously (von Gall et al. 1998). Young *mPer1*$^{-/-}$ *mCry2*$^{-/-}$ animals tended to show a slight (but statistically not significant) reduction in phosphorylation of CREB-Ser^{133} (Fig. 4C,D). In contrast, old *mPer1*$^{-/-}$ *mCry2*$^{-/-}$ mice hardly displayed phosphorylation at CREB-Ser^{133} ($p < 0.001$; Fig. 4C,D), suggesting a degeneration of the light input pathway to the clock.

Given the aberrant light-mediated *mPer2* mRNA induction and CREB-Ser^{133} phosphorylation in *mPer1*$^{-/-}$ *mCry2*$^{-/-}$ mice, we next wanted to investigate whether this had behavioral consequences. We monitored wheel-running activity before and after a 15-min light pulse at ZT14 or ZT22 as well as at CT14 or CT22 and measured the magnitude of phase shifts (Fig. 4E,F). In wild-type animals, we observed a phase delay at ZT14 of 82 ± 10 min (mean ± S.D., $n = 14$) and 87.3 ± 9.3 min ($n = 14$) at CT14 and a phase advance of 35 ± 6.7 min ($n = 14$) at ZT22 and 39.3 ± 6.7 min ($n = 14$) at CT22. In *mPer1*$^{-/-}$ *mCry2*$^{-/-}$ animals, only the phase shifts for young animals could be determined because the arrhythmicity of old *mPer1*$^{-/-}$ *mCry2*$^{-/-}$ animals in DD precludes such experiments. *mPer1*$^{-/-}$ *mCry1*$^{-/-}$ mice delayed their phase at ZT14 similar to wild-type animals (86.5 ± 12 min; $n = 11$; Fig. 4E). Remarkably, in *mPer1*$^{-/-}$ *mCry2*$^{-/-}$ mice, phase delays at CT14 tended to be reduced (60 ± 13 min; with $p = 0.0539$, $n = 10$), missing the criterion of $p < 0.05$ for significance (Fig. 4F). However, at ZT22 and CT22 phase advances in both *mPer1/mCry1* (1.3 ± 13 min; $n = 11$) and *mPer1/mCry2* (7.3 ± 10.5 min; $n = 10$), double-mutant animals were abolished (Fig. 4E,F), which is comparable to the inability of *mPer1*$^{-/-}$ mice to advance clock phase after a 15-min light pulse (Albrecht et al. 2001). These results suggest that the defect in advancing clock phase is caused by a lack of *mPer1* in both *mPer1*$^{-/-}$ *mCry1*$^{-/-}$ and *mPer1*$^{-/-}$ *mCry2*$^{-/-}$ mice. The impairment of delaying clock phase in *mPer1*$^{-/-}$ *mCry2*$^{-/-}$ mice at CT14 is probably caused by a reduction of phosphorylation in CREB-Ser^{133} and reduced expression of *mPer2* mRNA. This is in line with previous findings that *mPer2* mutant mice are defective in delaying clock phase (Albrecht et al. 2001).

CREB phosphorylation at Ser 133 is decreased in the eye of mPer1$^{-/-}$ mCry2$^{-/-}$ *mice*

The sloppy onset of wheel-running activity in LD and the strong reduction in CREB phosphorylation at Ser 133 in the SCN of old *mPer1*$^{-/-}$ *mCry2*$^{-/-}$ mice indicated that light signaling from the eye to the SCN might be defective. We therefore performed a histochemical analysis of the retina from wild-type, *mPer1*$^{-/-}$, *mCry2*$^{-/-}$, and *mPer1*$^{-/-}$ *mCry2*$^{-/-}$ mice, respectively (Fig. 5). No overt morphological differences between the retinas of these mice or cell death could be detected (Fig. 5A,B). Thus, the observed effects of aging in *mPer1*$^{-/-}$ *mCry2*$^{-/-}$ animals appear restricted to the functionality of the circadian system and are not likely to originate from aberrant development or age-related morphological changes in the retina.

Next we investigated phosphorylation of CREB at serine residue 133 in the retina by using an anti-Ser^{133} P-CREB antibody (Fig. 5C). In wild-type animals, in the absence of light stimuli, Ser^{133} P-CREB was detected in the inner nuclear layer. A light pulse given at ZT14 has been shown to result in increased numbers of immunoreactive nuclei in the inner nuclear layer and ganglion cell layer (Gau et al. 2002). In *mPer1*$^{-/-}$ and *mCry2*$^{-/-}$ single-mutant animals and in young *mPer1*$^{-/-}$ *mCry2*$^{-/-}$ mice, a similar immunoreactivity was seen (Fig. 5C). Old *mPer1*$^{-/-}$ *mCry2*$^{-/-}$ animals, however, displayed a reduced number of immunoreactive nuclei in the inner nuclear layer after a light pulse, whereas Ser^{133} P-CREB

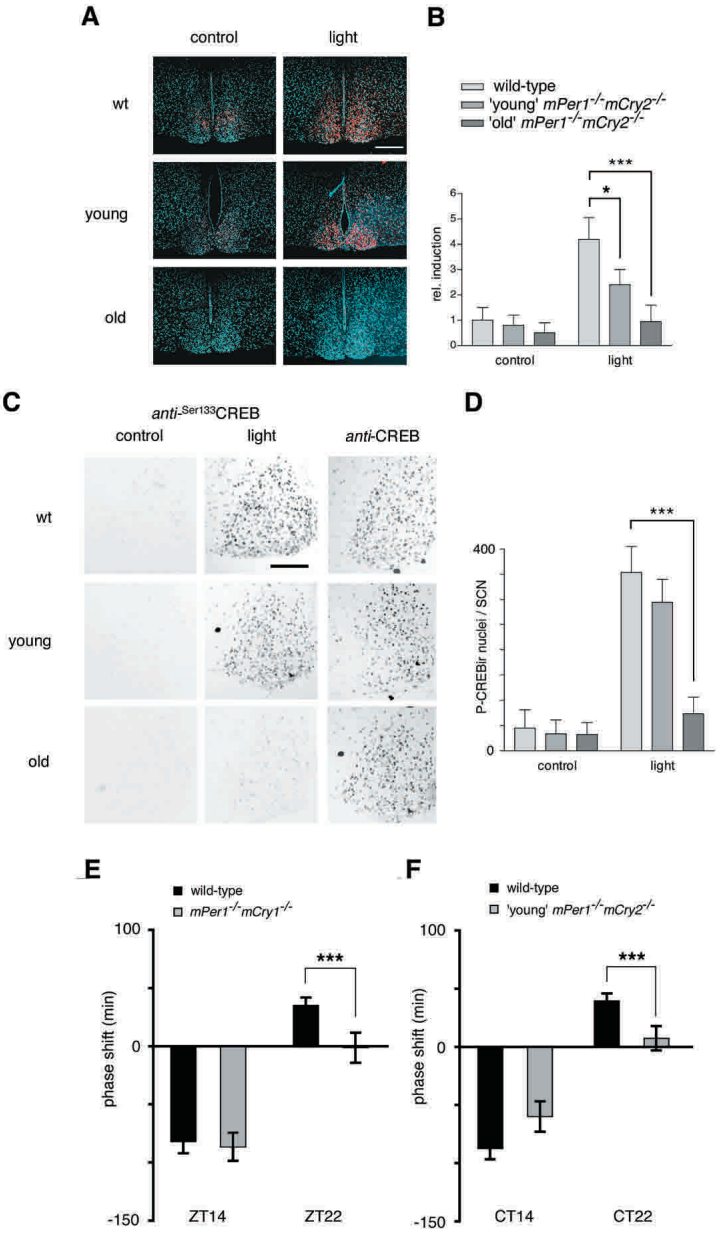

Figure 4. Light responsiveness in the SCN of young and old *mPer1*$^{-/-}$ *mCry2*$^{-/-}$ mice. (*A*) In situ hybridization analysis of *mPer2* light inducibility in the SCN of wild-type (wt, *top* row), young *mPer1*$^{-/-}$ *mCry2*$^{-/-}$ (*middle* row), and old *mPer1*$^{-/-}$ *mCry2*$^{-/-}$ mice (*bottom* row). Shown are representative micrographs of SCN probed with an *mPer2* antisense probe with (light) or without light administration (control) at ZT14 (15-min light pulse, 400 lx; animals were sacrificed 1 h later). Tissue was visualized by Hoechst dye nuclear staining (blue); silver grains are artificially colored (red) for clarification. Bar, 200 µm. (*B*) Quantification of *mPer2* induction after a light pulse at Z14. (*Left* panel) Control animals without light exposure. (*Right* panel) Relative *mPer2* mRNA induction after light exposure (wild-type control was set as 1). Data presented are mean ± S.D. of three different animals each. Statistical significance is indicated by asterisks (*, $p < 0.05$; ***, $p < 0.001$). (*C*) Immunohistochemistry analysis of CREB Ser 133 phosphorylation by light in the SCN of wild-type (wt, *top* row), young *mPer1*$^{-/-}$ *mCry2*$^{-/-}$ (*middle* row), and old *mPer1*$^{-/-}$ *mCry2*$^{-/-}$ mice (*bottom* row). Shown are representative micrographs of SCN sections immunostained for ^{Ser133}P-CREB with (light) or without light administration (control) at ZT14. As a control, SCN sections for all genotypes were stained for CREB (unphosphorylated) at the same time points. (*D*) Quantification of CREB phosphorylation after a light pulse at ZT14. Panels show numbers of ^{Ser133}P-CREB immunoreactive nuclei in the SCN with or without light exposure (***, $p < 0.001$). (*E*) Light-induced phase shifts in *mPer1*$^{-/-}$ *mCry1*$^{-/-}$ mice using the Aschoff Type II protocol to assess phase shifts. Animals were kept for at least 10 d in LD and released into DD after a light pulse at ZT14 or ZT22. Negative values indicate phase delays; positive values indicate phase advances. The data presented are mean ± S.D. of 10–14 animals (***, $p < 0.001$). (*F*) Light-induced phase shifts in young *mPer1*$^{-/-}$ *mCry2*$^{-/-}$ mice using the Aschoff Type I protocol to assess phase shifts. Animals were kept for at least 10 d in DD before a light pulse at CT14 or CT22. Data presented are mean ± S.D. of 10–13 animals.

staining could hardly be observed in the ganglion cell layer (Fig. 5C). Taken together, these results indicate that the profound loss of circadian wheel-running behavior of old *mPer1*$^{-/-}$ *mCry2*$^{-/-}$ mice under LD conditions (Fig. 1F) is caused by impaired light signal transduction pathway performance in combination with an age-related decline in core oscillator function.

Discussion

Interaction of clock components has predominantly been investigated in vitro (Gekakis et al. 1998; Kume et al. 1999; Yagita et al. 2000, 2002), revealing that mPER and mCRY proteins can form complexes that influence nuclear transport or regulate transcription of clock components. In contrast, it is not known to what extent complexes composed of various combinations of mPER and mCRY proteins contribute to circadian oscillator performance in vivo. We thus started to conduct genetic experiments by crossing mouse strains with inactivated *mPer* or *mCry* genes and subsequently analyzing circadian behavior, clock gene, and protein expression.

mPer1$^{-/-}$ mCry1$^{-/-}$ *mice display normal circadian rhythmicity but show impaired ability to phase advance the clock*

We have shown that *mPer1*$^{-/-}$ *mCry1*$^{-/-}$ mice, in contrast to short-period *mCry1*$^{-/-}$ mice, display a period length comparable to that of wild-type littermates (Fig.

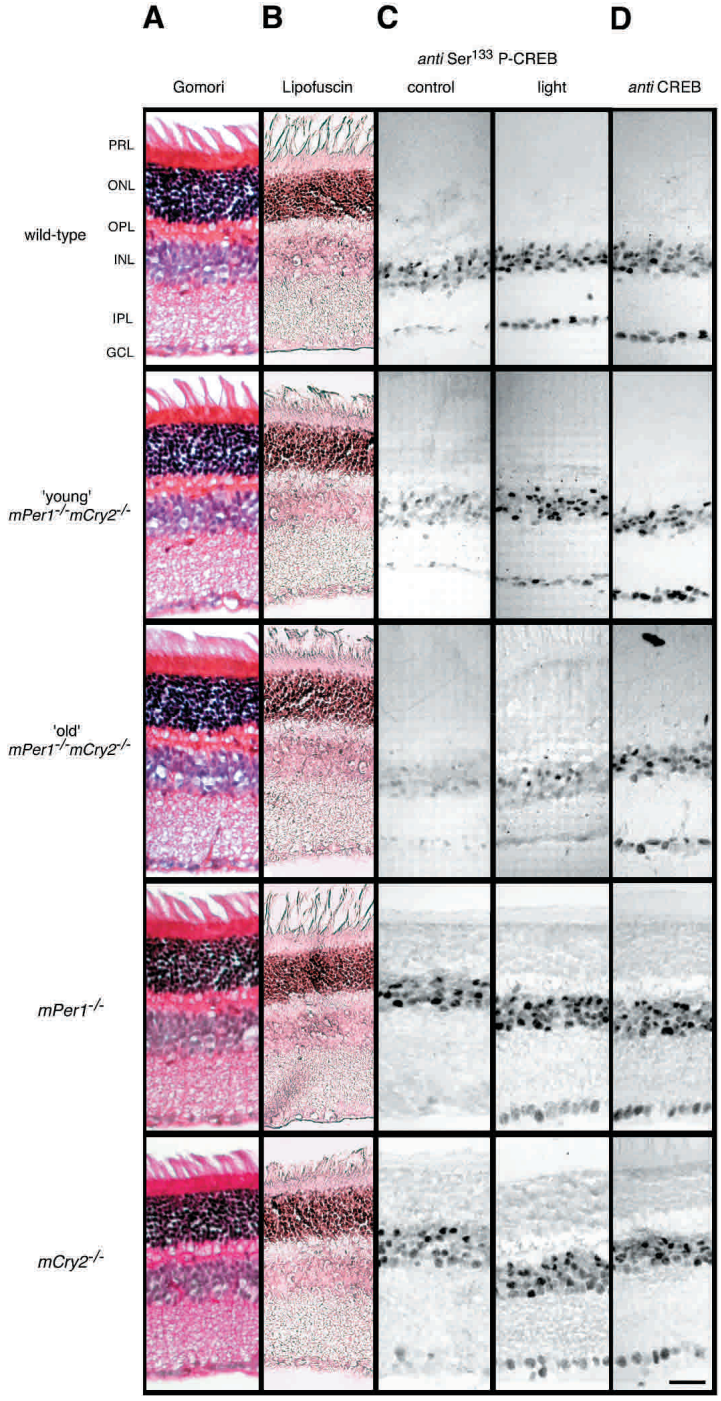

Figure 5. Histology and light responsiveness in the retina of wild-type, young, and old $mPer1^{-/-}$ $mCry2^{-/-}$ mice. Gomori trichrome (*A*) and lipofuscin (*B*) staining of retinal sections of wild-type (*first* row), young $mPer1^{-/-}$ $mCry2^{-/-}$ (*second* row), old $mPer1^{-/-}$ $mCry2^{-/-}$ (*third* row), $mPer1^{-/-}$ (*fourth* row), and $mCry2^{-/-}$ mice (*fifth* row). Retinal layers are indicated on the *left*. PRL, potoreceptor layer; ONL, outer nuclear layer; OPL, outer plexiform layer; INL, inner nuclear layer; IPL, inner plexiform layer; GCL, ganglion cell layer. (*C*) Immunohistochemistry analysis of light-induced CREB Ser 133 phosphorylation in the retina. (*Left* panels) Immunostained retinal sections of control animals without light exposure. (*Right* panels) Animals 1 h after light exposure (400 lx, 15 min) at ZT14. (*D*) Immunohistochemistry analysis for (unphosphorylated) CREB in the retina at ZT14. Bar, 10 µm.

1B,C). Thus, the additional loss of *mPer1* in $mCry1^{-/-}$ mice leads to an increase in period length to near normal values in DD (23.7 ± 0.2 h for $mPer1^{-/-}$ $mCry1^{-/-}$ mice vs. 22.51 ± 0.06 h for $Cry1^{-/-}$ mice). This also indicates that expression of the mPER2 and mCRY2 proteins apparently is sufficient to maintain circadian rhythmicity. The rescue of the $mCry1^{-/-}$ phenotype by additional loss of the *mPer1* gene is also reflected at the molecular level, where *mPer2* and *Bmal1* show normal mRNA rhythms under both LD and DD conditions (see Supplementary Fig. 1). Hence *mPer1* acts as a nonallelic suppressor of *mCry1*. Interestingly, $mPer1^{-/-}$ $mCry1^{-/-}$ animals could not phase advance their behavioral rhythms after a 15-min light pulse given at ZT22 (Fig. 4E), and in this respect resemble $mPer1^{-/-}$ animals (Albrecht et al. 2001). In conclusion, only circadian core clock functionality is rescued by an inactivation of *mCry1* in $mPer1^{-/-}$ mice, but not the resetting properties of the clock.

Breakdown of the clock in aging mPer1$^{-/-}$ mCry2$^{-/-}$ *mice*

Circadian organization changes with age (Valentinuzzi et al. 1997; Yamazaki et al. 2002). Typical changes include decrease in the amplitude of wheel-running activity, fragmentation of the activity rhythm, decreased precision in onset of daily activity, and alterations in the response to the phase-shifting effects of light (Valentinuzzi et al. 1997). In mice, aging has been found to diminish the amplitude of *Per2* but not *Per1* expression (Weinert et al. 2001).

Here, we provide evidence that a clock defect can make the circadian oscillator fall apart more quickly, resembling accelerated aging. Inactivation of *mPer1* and *mCry2* in young *mPer1*$^{-/-}$ *mCry2*$^{-/-}$ mice (2–6 mo old) leads to a decreased precision in onset of daily activity (Fig. 1D,E). Additionally, onset of activity is markedly delayed, with a sharp offset at the dark/light transition probably reflecting masking (Mrosovsky 1999). In old *mPer1*$^{-/-}$ *mCry2*$^{-/-}$ mice, the precision in onset of daily activity is even further deteriorated (Fig. 1F). Moreover, animals start to display fragmentation of activity under LD conditions, and daily rhythms become barely detectable (Fig. 1G). In constant darkness, old *mPer1*$^{-/-}$ *mCry2*$^{-/-}$ mice no longer display circadian rhythmicity, and the amplitude of wheel-running activity is decreased compared with that of wild-type and young *mPer1*$^{-/-}$ *mCry2*$^{-/-}$ mice (Fig. 1F,I). The percentage of arrhythmic *mPer1*$^{-/-}$ *mCry2*$^{-/-}$ mice increases with age (Fig. 1H), but the time of onset of the arrhythmic circadian phenotype varies among animals, indicating that additional genes or genetic background may contribute to the aging process. All these features are observed neither in *mPer1*$^{-/-}$ and *mCry2*$^{-/-}$ single-mutant mice (van der Horst et al. 1999; Zheng et al. 2001; Supplementary Fig. 2) nor in *mPer1*$^{-/-}$ *mCry1*$^{-/-}$, *mPer2*^{Brdm1} *mCry1*$^{-/-}$, *mPer2*^{Brdm1} *mCry2*$^{-/-}$ (Supplementary Fig. 2D), or heterozygous *mPer1 mCry1* and *mPer1 mCry2* mice (Supplementary Fig. 4).

Gene expression is known to change upon aging. Alterations in mRNA and protein levels can result from changes in transcriptional regulation (Roy et al. 2002), mRNA stability (Brewer 2002), and proteasome-mediated protein degradation (Goto et al. 2001). We have shown that the absence of *mPer1* and *mCry2* specifically alters the regulation of the circadian core oscillator in an age-related manner. This is illustrated by our observation that *mPer2* and *Bmal1* mRNA levels are strongly reduced in the SCN and in the kidney of old *mPer1*$^{-/-}$ *mCry2*$^{-/-}$ mice (Figs. 2, 3E,F). Additionally, mCRY1 protein levels are elevated (Fig. 3C), pointing to an impaired degradation of mCRY1 protein. Interestingly, *mCry1* mRNA cycling is not affected in contrast to *mPer2* and *Bmal1* transcripts, indicating that regulation of *mCry1* differs from that of *mPer2* and *Bmal1*. Old *mPer1*$^{-/-}$ *mCry2*$^{-/-}$ mice display not only altered gene expression of core clock components but also altered expression of the clock output gene arginine-vasopressin (*Avp*; Fig. 3G), indicating that physiological pathways influenced by *Avp* are affected in these mice. Interestingly, *Dbp* seems to be regulated differently, because its gene expression is already altered in *mCry2*$^{-/-}$ mice (Fig. 3H; Supplementary Fig. 3H).

Light sensitivity is impaired in aging mPer1$^{-/-}$ mCry2$^{-/-}$ *mice*

Old *mPer1*$^{-/-}$ *mCry2*$^{-/-}$ mice synchronize poorly to the light dark cycle (Fig. 1F). Therefore, we tested whether CREB, an essential factor for numerous transcriptional processes, was activated by phosphorylation in response to a light pulse (Motzkus et al. 2000; Travnickova-Bendova et al. 2002). CREB phosphorylation was only slightly lowered in young *mPer1*$^{-/-}$ *mCry2*$^{-/-}$ mice but was significantly impaired in old animals (Fig. 4C,D), indicating a defect in light signaling in the SCN of these mice. At the behavioral level, we could only measure the phase shifts of young *mPer1*$^{-/-}$ *mCry2*$^{-/-}$ mice, because old animals immediately became arrhythmic in DD. The young *mPer1*$^{-/-}$ *mCry2*$^{-/-}$ mice resemble *mPer1*$^{-/-}$ animals in that they were not able to advance clock phase (Fig. 4F; Albrecht et al. 2001), suggesting that this anomaly is due to the absence of *mPer1*.

The impaired light response of *mPer1*$^{-/-}$ *mCry2*$^{-/-}$ mice might be a consequence of a defect in transmitting light information from the eye to the SCN. To test this possibility, we looked for anatomical malformations in the retina. Neither young nor old *mPer1*$^{-/-}$ *mCry2*$^{-/-}$ mice displayed overt abnormalities in retinal morphology (Fig. 5A). Cell death as a reason for malfunction of the retina could most possibly be excluded, because lipofuscin staining (Fig. 5B) and Congo red staining (data not shown) did not reveal dead cells in the retina. Comparable to the SCN, however, light-dependent phosphorylation of CREB at Ser 133 was affected in old *mPer1*$^{-/-}$ *mCry2*$^{-/-}$ mice (Fig. 5C). As a consequence, light perceived by the eye is probably not processed properly to induce cellular signaling. The reason for the impaired transmission of the light signal is most likely not a developmental defect, because young *mPer1*$^{-/-}$ *mCry2*$^{-/-}$ mice show phosphorylation of CREB at Ser 133. Therefore, the defect is probably of transcriptional or posttranscriptional nature. The lack of phosphorylation of CREB might lead to an altered expression of melanopsin in ganglion cells. These cells are probably responsible for resetting of the clock by light (Berson et al. 2002; Hattar et al. 2002). Hence, a reduced expression of melanopsin would affect resetting. This is in line with the recent finding, that melanopsin-deficient mice display attenuated clock resetting in response to brief light pulses (Panda et al. 2002; Ruby et al. 2002), similar to what we observe in *mPer1*$^{-/-}$ *mCry2*$^{-/-}$ mice (Fig. 4F). In old *mPer1*$^{-/-}$ *mCry2*$^{-/-}$ mice, this might even lead to the poor synchronization of these mice to the LD cycle (Fig. 1F,G). Future studies will reveal whether melanopsin expression in ganglion cells of the retina is affected in old *mPer1*$^{-/-}$ *mCry2*$^{-/-}$ mice.

The transcriptional potential of mPER and mCRY protein complexes and their temporal abundance determines circadian rhythmicity

The precise regulation of the circadian oscillator requires an exact choreography of clock protein synthesis, interaction, posttranslational modification, and nuclear localization (Lee et al. 2001; Yagita et al. 2002). The positive limb of circadian clock gene activation is influenced by the negative limb via REV-ERBα (Preitner et al. 2002), probably through a complex consisting of mPER and mCRY proteins (Albrecht 2002; Okamura et al. 2002; Yu et al. 2002). The mPER and mCRY proteins stabilize each other when they are in a complex and inhibit the CLOCK/BMAL1 heterodimer. Such a mPER/mCRY complex would be composed of those PER and CRY proteins that are most abundant at a given time. Figure 6A depicts the temporal abundance of cycling *mPer1*, *mPer2*, *mCry1*, and *mCry2* mRNA in the SCN, illustrating that the amount of mRNA of these genes differs with time (Albrecht et al. 1997; Okamura et al. 1999; Reppert and Weaver 2002; Yan and Okamura 2002). Because the clock components of the negative limb (*Per* and *Cry*) are regulating their own transcription, the mRNA cycling is likely to reflect the activity of the corresponding proteins. The active forms of PER and CRY proteins seem to be cycling with a delay of 4–6 h compared with mRNA (Field et al. 2000).

Interestingly, not all PER/CRY complexes seem to be equally important in vivo (Oster et al. 2002; this study). $mPer2^{Brdm1}$ $mCry2^{-/-}$ mutant but not $mPer2^{Brdm1}$ $mCry1^{-/-}$ mutant mice display circadian rhythmic behavior, indicating that mPER1/mCRY1 but not mPER1/mCRY2 is sufficient to drive the circadian clock (Oster et al. 2002). This study indicates that mPER2/mCRY2 but—at least in older mice—not mPER2/mCRY1 can sustain circadian rhythms. Additionally, $mPer1^{-/-}$ $mPer2^{Brdm1}$ and $mCry1^{-/-}$ $mCry2^{-/-}$ double-mutant mice do not show circadian rhythmicity, indicating that mPER or mCRY homodimers are not sufficient to maintain circadian rhythmicity. Based on these observations, we propose activity and timing of PER/CRY complexes as illustrated in Figure 6B. According to this model, the complexes composed of mPER1/mCRY1 and mPER2/mCRY2 would be the most active ones, with a difference in their maxima of ~2 h. The activity of these complexes is higher than a critical threshold level necessary to drive clock regulation (green horizontal line in Fig. 6B). In contrast, mPER1/mCRY2 complexes formed in *Per2*/*Cry1* mutant mice probably do not reach this critical threshold. The reason for this might be that the timing of expression of these two proteins is not synchronized and/or the affinity between mPER1 and mCRY2 is low. As a consequence, *Per2*/*Cry1* mutant mice lose clock function (Oster et al. 2002). The complex containing mPER2 and mCRY1 seems to just reach the critical threshold necessary for clock regulation, as illustrated by the circadian wheel-running behavior of young $mPer1^{-/-}$ $mCry2^{-/-}$ mice (Fig. 1D,E). However, with progressing age, the activity of such a complex falls below the threshold, and hence, older $mPer1^{-/-}$ $mCry2^{-/-}$ mice lose rhythmicity (Fig. 1F,I). $mPer2^{Brdm1}$ mutant mice lose circadian rhythmicity after a few days in constant darkness. In these animals only functional mPER1/mCRY1 and

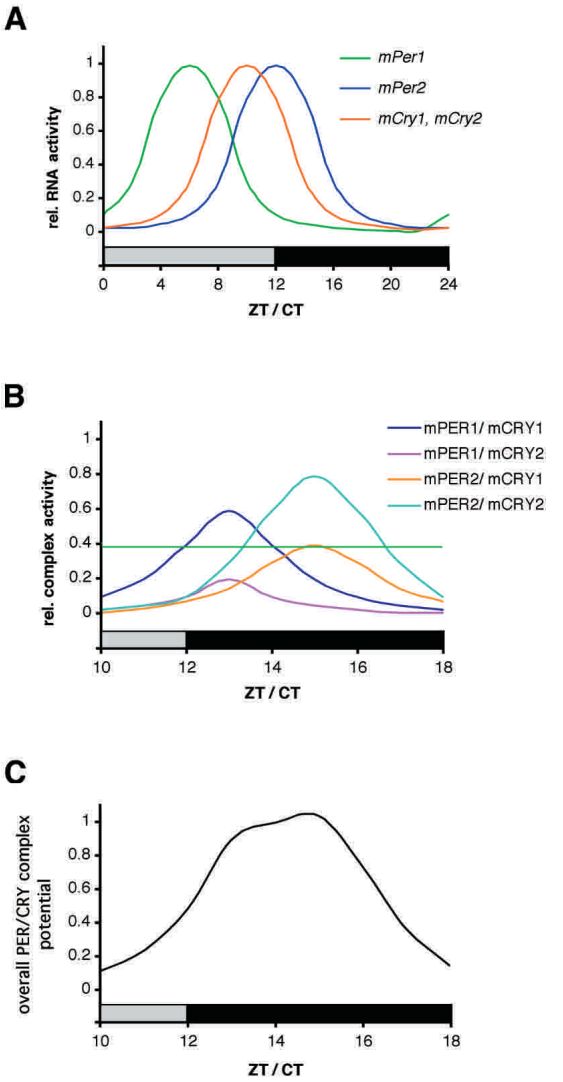

Figure 6. Working model for PER/CRY-driven inhibition of CLOCK/BMAL1. (*A*) *mPer* and *mCry* transcripts show diurnal/circadian cycling in the SCN. Whereas *mPer1* expression peaks between ZT/CT 4 and 8, *mCry1* and *mPer2* mRNA rhythms have their maxima at ZT/CT10 to ZT/CT12, respectively. Note that *mCry2* is also expressed in the SCN but without a clearly defined rhythm. Protein peaks are delayed by ~4–6 h with regard to mRNA. (*B*) mPER and mCRY proteins form heteromeric complexes that form with certain preferences according to protein–protein affinity and temporal abundance. The complexes are color coded, with mPER1/mCRY1 and mPER2/mCRY2 representing the most abundant ones. The green horizontal line indicates a threshold above which a PER/CRY complex is abundant enough to influence CLOCK/BMAL1 transcription. (*C*) Time course of the overall inhibitory potential of the mPER/mCRY heteromers on CLOCK/BMAL1 activity. The strong inhibition of CLOCK/BMAL1 during (subjective) night corresponds to the low transcriptional activity of (CLOCK/BMAL1-induced) *mPer* and *mCry* genes.

mPER1/mCRY2 complexes can form, which should in principle be sufficient to drive a circadian rhythm. This seems to be the case for the first few days in constant darkness, but then competition between mCRY1 and mCRY2 for PER1 could lead to equal amounts of PER1/CRY1 and PER1/CRY2 complexes. The activity of each of these complexes might then fall below the threshold critical for normal clock function.

In sum, it seems that PER/CRY complexes have different potentials to regulate the circadian clock. In wild-type animals, the formation of PER/CRY complexes is not random and depends on temporal abundance and strength of interaction between the complex-forming partners (Fig. 6B). The sum of the regulatory potential of PER/CRY complexes over time displays a robust circadian cycling, as illustrated in Figure 6C. The robustness of this cycling may be ensured by the different phasing of the oscillation of the two strong regulatory complexes PER1/CRY1 and PER2/CRY2. This notion is supported by theoretical considerations indicating that an overt oscillation is stabilized by two oscillators that are slightly out of phase (Glass and Mackey 1988; Roenneberg and Merrow 2001). Our findings are also in agreement with the two-oscillator model proposed by Daan and coworkers (2001).

Taken together, our in vivo studies support a model based on differential presence and activity of PER/CRY protein complexes as critical regulators of circadian rhythmicity (Fig. 6). It is reasonable to conclude that not all interactions between PER and CRY proteins are equal in vivo. Although these proteins seem to be partially redundant, all of them are necessary for a functional circadian clock that can predict time and thereby be adaptable to changing environmental conditions. The importance of PER1 and CRY2 only becomes apparent in *mPer1*$^{-/-}$ *mCry2*$^{-/-}$ mice half a year after birth, illustrating a connection between the clock and aspects of aging.

Materials and methods

Generation of mPer *and* mCry *mutant mice*

We crossed *mPer1*$^{-/-}$ mice (Zheng et al. 2001) with *mCry1*$^{-/-}$ and *mCry2*$^{-/-}$ animals (van der Horst et al. 1999). The genotype of the offspring was determined by Southern blot analysis as described (Oster et al. 2002). Hybridization probes were for *mPer1* as described in Zheng et al. (2001) and for *mCry1* and *mCry2* as described in van der Horst et al. (1999). Matching wild-type control animals were produced by back-crossing heterozygous animals derived from the *mPer1*$^{-/-}$ and *mCry*$^{-/-}$ matings to minimize epigenetic effects.

Locomotor activity monitoring and circadian phenotype analysis

Mice housing and handling were performed as described (Albrecht and Oster 2001; Albrecht and Foster 2002). For LD–DD transitions, lights were turned off at the end of the light phase and not turned on again the next morning. Activity records are double plotted so that each light/dark cycle's activity is shown both to the right and below that of the previous light/dark cycle. Activity is plotted in threshold format for 5-min bins. For activity counting and evaluation, we used the ClockLab software package (Actimetrics). Rhythmicity and period length were assessed by χ^2 periodogram analysis and Fourier transformation using mice running in LD or in DD for at least 10 d.

For light-induced phase shifts, we used the Aschoff Type I (for *mPer1*$^{-/-}$ *mCry1*$^{-/-}$ animals) or the Type II protocol (for *mPer1*$^{-/-}$ *mCry2*$^{-/-}$ animals) as described (Albrecht and Oster 2001; Albrecht et al. 2001). We originally chose the Type II protocol because of the convenient setup for high numbers of animals and for comparison with *mPer2*^{Brdm1} mice (Albrecht et al. 2001; Oster et al. 2002). However, the unstable onset of activity of *mPer1*$^{-/-}$ *mCry2*$^{-/-}$ mice in LD and the long period length of these animals in DD resulted in very high variations when determining the phase shifts with the Type II protocol. Therefore, we repeated the experiments using a Type I setup with animals free running in DD before light administration. For the Type II protocol, animals were entrained to an LD cycle for at least 7 d before light administration (15 min of bright white light, 400 lx, at ZT14 or ZT22) and subsequently released into DD. The phase shift was determined by drawing a line through at least 7 consecutive days of onset of activity in LD before the light pulse and in DD after the light pulse as determined by the ClockLab program. The difference between the two lines on the day of the light pulse determined the value of the phase shift. For the Type I protocol, animals were kept in DD for at least 10 d before the light pulse (at CT14 or CT22, respectively). The phase shift was determined by drawing lines through at least 7 consecutive days before and after the light pulse using the ClockLab software. The first 1 or 2 d following the light administration were not used for the calculation because animals were thought to be in transition between both states.

In situ hybridization

Mice were sacrificed by cervical dislocation under ambient light conditions at ZT6 and ZT12 and under a 15W safety red light at ZT18 and ZT0/24 as well as at CT0/24, 6, 12, and 18. For DD conditions, animals were kept in the dark for 3 d before decapitation. For light induction experiments, animals were exposed to a 15-min light pulse (400 lx) at ZT14 and killed at ZT15; controls were killed at ZT15 without prior light exposure. Specimen preparation, ^{35}S-rUTP-labeled riboprobe synthesis, and hybridization steps were performed as described (Albrecht et al. 1998). The probe for *mPer2* was as described (Albrecht et al. 1997). The *mCry1* and the *Bmal1* probes were as described (Oster et al. 2002). The *Dbp* probe was made from a cDNA corresponding to nucleotides 2–951 (GenBank accession no. NM016974). The vasopressin (*Avp)* probe corresponds to nucleotides 1–480 (GenBank accession no. M88354). Quantification was performed by densitometric analysis of autoradiograph films (Amersham Hyperfilm MP) as described (Oster et al. 2002). For each time point, three animals were used and three sections per SCN were analyzed. "Relative mRNA abundance" values were calculated by defining the highest value of each experiment as 100%.

Immunohistochemistry

Animals were killed and tissues were prepared as described for in situ hybridization. Eye lenses were removed before cutting. Sections were boiled in 0.01 M sodium citrate (pH 6) for 10 min to unmask hidden antigen epitopes and were processed for immunohistochemical detection using the Vectastain Elite ABC system (Vector Laboratories) and diaminobenzidine with nickel

amplification as the chromogenic substrate. Immunostained sections were inspected with an Axioplan microscope (Zeiss), and the area of the SCN was determined by comparison to Nissl-stained parallel sections. Semiquantitative analysis for mCRY1, mPER2, and ^{Ser133}P-CREB immunoreactivity in the SCN was performed using the NIH Image program. Images were digitized; background staining was used to define a lower threshold. Within the whole area of the SCN, all cell nuclei exceeding the threshold value were marked. Three sections of the intermediate aspect of the SCN were chosen at random for further analysis. Values presented are the mean of three different experiments ±S.D. Primary antibodies against mCRY1 (Alpha Diagnostics, order number CRY11-A), against CREB (Cell Signaling Technology, order no. 9192), against CREB, phosphorylated at the residue Ser 133 (New England Biolabs, order no. 9191S), and against mPER2 (Santa Cruz Biotechnology, order no. sc-7729) were used at dilutions of 1:200, 1:500, 1:1000, and 1:200, respectively.

Northern blot analysis

Rhythmic animals were sacrificed at the specified time points. Total RNA from kidney was extracted using RNAzol B (WAK Chemie). Northern analysis was performed using denaturing formaldehyde gels (Sambrook and Russell 2001), with subsequent transfer to Hybond-N$^+$ membrane (Amersham). For each sample, 20 µg of total RNA was used. cDNA probes were the same as described for in situ hybridization. Labeling of probes was done using the Rediprime II labeling kit (Pharmacia) incorporating [^{32}P]dCTP to a specific activity of 10^8 cpm/µg. Blots were hybridized using UltraHyb solution (Ambion) containing 100 µg/mL salmon sperm DNA. The membrane was washed at 60°C in 0.1× SSPE and 0.1% SDS. Subsequently, blots were exposed to phosphoimager plates (Bio-Rad) for 20 h, and signals were quantified using Quantity One 3.0 software (Bio-Rad). For comparative purposes, the same blot was stripped and reused for hybridization. The relative level of RNA in each lane was determined by hybridization with mouse *Gapdh* cDNA.

Histology

All histological staining was performed as described (Burkett et al. 1993). For Gomori's trichrome staining, PFA-fixed, paraffin-embedded sections were dewaxed, and postfixed with Bouin's fluid at 56°C for 30 min; nuclei were stained with ferric haematoxyline (according to Weigert) for 10 min. After washing in water, slides were incubated for 15 min with trichrome stain [Chromotrope 2R, 0.6% (w/v), and Light Green, 0.3% (w/v), in 1% (v/v) acetic acid and 0.8% (w/v) phosphotungstic acid]. After washing with 0.5% acetic acid and 1% (v/v) acetic acid/0.7% (w/v) phosphotungstic acid, slides were rinsed with water, dehydrated, and mounted with Canada balsam/methyl salycilate.

For lipofuscin staining, slides were dewaxed and colored with 0.75% (w/v) ferric chloride/0.1% (w/v) potassium ferricyanide (Aldrich) for 5 min. After washing with 1% (v/v) acetic acid and water, slides were incubated with 1% (w/v) Neutral Red for 3–4 min and subsequently washed with water, dehydrated, and mounted with Dpx mounting media (Fluka). All reagents were from Sigma if not stated otherwise.

Statistical analysis

Statistical analysis of all experiments was performed using GraphPad Prism software (GraphPad). Significant differences between groups were determined with one-way ANOVA, followed by Bonferroni's *post*-test. Values were considered significantly different with $p < 0.05$ (*), $p < 0.01$ (**), or $p < 0.001$ (***).

Acknowledgments

This work was supported by a SPINOZA premium from the Netherlands Organisation for Scientific Research (NWO) to G.T.J.v.d.H. and the Swiss National Science Foundation, the State of Fribourg, the Novartis Foundation, the AETAS Foundation for Research into Aging, and the Hans Wilsdorf Foundation in Geneva to U.A. This research has been part of the BrainTime project (QLRT-2001-01829) funded by the European Community and the Swiss Office for Education and Research.

The publication costs of this article were defrayed in part by payment of page charges. This article must therefore be hereby marked "advertisement" in accordance with 18 USC section 1734 solely to indicate this fact.

References

Albrecht, U. 2002. Invited Review: Regulation of mammalian circadian clock genes. *J. Appl. Physiol.* **92:** 1348–1355.

Albrecht, U. and Foster, R.G. 2002. Placing ocular mutants into a functional context: A chronobiological approach. *Methods* **28:** 465–477.

Albrecht, U. and Oster, H. 2001. The circadian clock and behavior. *Behav. Brain Res.* **125:** 89–91.

Albrecht, U., Sun, Z.S., Eichele, G., and Lee, C.C. 1997. A differential response of two putative mammalian circadian regulators, mper1 and mper2, to light. *Cell* **91:** 1055–1064.

Albrecht, U., Lu, H.-C., Revelli, J.-P., Xu, X.-C., Lotan, R., and Eichele, G. 1998. Studying gene expression on tissue sections using in situ hybridization. In *Human genome methods* (ed. K.W. Adolph), pp. 93–119. CRC Press, New York.

Albrecht, U., Zheng, B., Larkin, D., Sun, Z.S., and Lee, C.C. 2001. mper1 and mper2 are essential for normal resetting of the circadian clock. *J. Biol. Rhythms* **16:** 100–104.

Allada, R., Emery, P., Takahashi, J.S., and Rosbash, M. 2001. Stopping time: The genetics of fly and mouse circadian clocks. *Annu. Rev. Neurosci.* **24:** 1091–1119.

Bae, K., Jin, X., Maywood, E.S., Hastings, M.H., Reppert, S.M., and Weaver, D.R. 2001. Differential functions of *mPer1*, *mPer2*, and *mPer3* in the SCN circadian clock. *Neuron* **30:** 525–536.

Balsalobre, A., Damiola, F., and Schibler, U. 1998. A serum shock induces circadian gene expression in mammalian tissue culture cells. *Cell* **93:** 929–937.

Berson, D.M., Dunn, F.A., and Takao, M. 2002. Phototransduction by retinal ganglion cells that set the circadian clock. *Science* **295:** 1070–1073.

Brewer, G. 2002. Messenger RNA decay during aging and development. *Ageing Res. Rev.* **1:** 607–625.

Burkett, H.G., Young, B., and Heath, J.W. 1993. *Wheather's functional histology*, 3 ed. Churchill Livingstone, London.

Cermakian, N., Monaco, L., Pando, M.P., Dierich, A., and Sassone-Corsi, P. 2001. Altered behavioral rhythms and clock gene expression in mice with a targeted mutation in the Period1 gene. *EMBO J.* **20:** 3967–3974.

Daan, S., Albrecht, U., van der Horst, G.T., Illnerova, H., Roenneberg, T., Wehr, T. A., and Schwartz, W.J. 2001. Assembling a clock for all seasons: Are there M and E oscillators in the genes? *J. Biol. Rhythms* **16:** 105–116.

Field, M.D., Maywood, E.S., O'Brien, J.A., Weaver, D.R., Reppert, S.M., and Hastings, M.H. 2000. Analysis of clock pro-

teins in mouse SCN demonstrates phylogenetic divergence of the circadian clockwork and resetting mechanisms. *Neuron* **25:** 437–447.

Gau, D., Lemberger, T., von Gall, C., Kretz, O., Le Minh, N., Gass, P., Schmid, W., Schibler, U., Korf, H.W., and Schutz, G. 2002. Phosphorylation of CREB Ser142 regulates light-induced phase shifts of the circadian clock. *Neuron* **34:** 245–253.

Gekakis, N., Staknis, D., Nguyen, H.B., Davis, F.C., Wilsbacher, L.D., King, D.P., Takahashi, J.S., and Weitz, C.J. 1998. Role of the CLOCK protein in the mammalian circadian mechanism. *Science* **280:** 1564–1569.

Glass, L. and Mackey, M.C. 1988. From clocks to chaos—The rhythms of life. Princeton University Press, Princeton, NJ.

Goto, S., Takahashi, R., Kumiyama, A.A., Radak, Z., Hayashi, T., Takenouchi, M., and Abe, R. 2001. Implications of protein degradation in aging. *Ann. NY Acad. Sci.* **928:** 54–64.

Hamada, T., LeSauter, J., Venuti, J.M., and Silver, R. 2001. Expression of period genes: Rhythmic and nonrhythmic compartments of the suprachiasmatic nucleus pacemaker. *J. Neurosci.* **21:** 7742–7750.

Hattar, S., Liao, H.W., Takao, M., Berson, D.M., and Yau, K.W. 2002. Melanopsin-containing retinal ganglion cells: Architecture, projections, and intrinsic photosensitivity. *Science* **295:** 1065–1069.

Honma, S., Ikeda, M., Abe, H., Tanahashi, Y., Namihira, M., Honma, K., and Nomura, M. 1998. Circadian oscillation of BMAL1, a partner of a mammalian clock gene Clock, in rat suprachiasmatic nucleus. *Biochem. Biophys. Res. Commun.* **250:** 83–87.

Jacob, N., Vuillez, P., Lakdhar-Ghazal, N., and Pevet, P. 1999. Does the intergeniculate leaflet play a role in the integration of the photoperiod by the suprachiasmatic nucleus? *Brain Res.* **828:** 83–90.

Jagota, A., de la Iglesia, H.O., and Schwartz, W.J. 2000. Morning and evening circadian oscillations in the suprachiasmatic nucleus in vitro. *Nat. Neurosci.* **3:** 372–376.

Kume, K., Zylka, M.J., Sriram, S., Shearman, L.P., Weaver, D.R., Jin, X., Maywood, E.S., Hastings, M.H., and Reppert, S.M. 1999. mCRY1 and mCRY2 are essential components of the negative limb of the circadian clock feedback loop. *Cell* **98:** 193–205.

Lee, C., Etchegaray, J.P., Cagampang, F.R., Loudon, A.S., and Reppert, S.M. 2001. Posttranslational mechanisms regulate the mammalian circadian clock. *Cell* **107:** 855–867.

Miyamoto, Y. and Sancar, A. 1998. Vitamin B2-based blue-light photoreceptors in the retinohypothalamic tract as the photoactive pigments for setting the circadian clock in mammals. *Proc. Natl. Acad. Sci.* **95:** 6097–6102.

Miyazaki, K., Mesaki, M., and Ishida, N. 2001. Nuclear entry mechanism of rat PER2 (rPER2): Role of rPER2 in nuclear localization of CRY protein. *Mol. Cell. Biol.* **21:** 6651–6659.

Motzkus, D., Maronde, E., Grunenberg, U., Lee, C.C., Forssmann, W., and Albrecht, U. 2000. The human PER1 gene is transcriptionally regulated by multiple signaling pathways. *FEBS Lett.* **486:** 315–319.

Mrosovsky, N. 1999. Masking: History, definitions, and measurement. *Chronobiol. Int.* **16:** 415–429.

Okamura, H., Miyake, S., Sumi, Y., Yamaguchi, S., Yasui, A., Muijtjens, M., Hoeijmakers, J.H., and van der Horst, G.T. 1999. Photic induction of mPer1 and mPer2 in cry-deficient mice lacking a biological clock. *Science* **286:** 2531–2534.

Okamura, H., Yamaguchi, S., and Yagita, K. 2002. Molecular machinery of the circadian clock in mammals. *Cell Tissue Res.* **309:** 47–56.

Oster, H., Yasui, A., van der Horst, G. T., and Albrecht, U. 2002. Disruption of *mCry2* restores circadian rhythmicity in *mPer2* mutant mice. *Genes & Dev.* **16:** 2633–2638.

Panda, S., Sato, T.K., Castrucci, A.M., Rollag, M.D., DeGrip, W.J., Hogenesch, J.B., Provenico, I., and Kay, S.A. 2002. Melanopsin (*Opn4*) requirement for normal light-induced circadian phase shifting. *Science* **298:** 2213–2216.

Pittendrigh, C.S. 1993. Temporal organization: Reflections of a Darwinian clock-watcher. *Annu. Rev. Physiol.* **55:** 16–54.

Preitner, N., Damiola, F., Lopez-Molina, L., Zakany, J., Duboule, D., Albrecht, U., and Schibler, U. 2002. The orphan nuclear receptor REV-ERBα controls circadian transcription within the positive limb of the mammalian circadian oscillator. *Cell* **110:** 251–260.

Ralph, M.R., Foster, R.G., Davis, F.C., and Menaker M. 1990. Transplanted suprachiasmatic nucleus determines circadian period. *Science* **247:** 975–978.

Reppert, S. and Weaver, D. 2002. Coordination of circadian timing in mammals. *Nature* **418:** 935–941.

Roenneberg, T. and Merrow, M. 2001. Circadian systems: Different levels of complexity. *Philos. Trans. R Soc. Lond. B Biol. Sci.* **356:** 1687–1696.

Roy, A.K., Oh, T., Rivera, O., Mubiru, J., Song, C.S., and Chatterjee, B. 2002. Impacts of transcriptional regulation on aging and senescence. *Ageing Res. Rev.* **1:** 367–380.

Ruby, N.F., Brennan, T.J., Xie, X., Cao, V., Franken, P., Heller, H.C., and O'Hara, B.F. 2002. Role of melanopsin in circadian responses to light. *Science* **298:** 2211–2213.

Rusak, B. and Zucker, I. 1979. Neural regulation of circadian rhythms. *Physiol. Rev.* **59:** 449–526.

Sambrook, J. and Russell, D.W. 2001. *Molecular cloning: A laboratory manual*, 3rd ed., Vol. 1. Cold Spring Harbor Laboratory Press, Cold Spring Harbor, NY.

Shearman, L.P., Zylka, M.J., Weaver, D.R., Kolakowski Jr., L.F., and Reppert, S.M. 1997. Two period homologs: Circadian expression and photic regulation in the suprachiasmatic nuclei. *Neuron* **19:** 1261–1269.

Shearman, L.P., Jin, X., Lee, C., Reppert, S.M., and Weaver, D.R. 2000. Targeted disruption of the mPer3 gene: Subtle effects on circadian clock function. *Mol. Cell. Biol.* **20:** 6269–6275.

Sun, Z.S., Albrecht, U., Zhuchenko, O., Bailey, J., Eichele, G., and Lee, C.C. 1997. RIGUI, a putative mammalian ortholog of the *Drosophila* period gene. *Cell* **90:** 1003–1011.

Tei, H., Okamura, H., Shigeyoshi, Y., Fukuhara, C., Ozawa, R., Hirose, M., and Sakaki, Y. 1997. Circadian oscillation of a mammalian homologue of the *Drosophila* period gene. *Nature* **389:** 512–516.

Travnickova-Bendova, Z., Cermakian, N., Reppert, S.M., and Sassone-Corsi, P. 2002. Bimodal regulation of mPeriod promoters by CREB-dependent signaling and CLOCK/BMAL1 activity. *Proc. Natl. Acad. Sci.* **14:** 14.

Valentinuzzi, V.S., Scarbrough, K., Takahashi, J.S., and Turek, F.W. 1997. Effects of aging on the circadian rhythm of wheel-running activity in C57BL/6 mice. *Am. J. Physiol.* **273:** R1957–R1964.

van der Horst, G.T., Muijtjens, M., Kobayashi, K., Takano, R., Kanno, S., Takao, M., de Wit, J., Verkerk, A., Eker, A.P., van Leenen, D., et al. 1999. Mammalian Cry1 and Cry2 are essential for maintenance of circadian rhythms. *Nature* **398:** 627–630.

Vielhaber, E.L., Duricka, D., Ullman, K.S., and Virshup, D.M. 2001. Nuclear export of mammalian PERIOD proteins. *J. Biol. Chem.* **8:** 8.

Vitaterna, M.H., Selby, C.P., Todo, T., Niwa, H., Thompson, C., Fruechte, E.M., Hitomi, K., Thresher, R.J., Ishikawa, T., Miyazaki, J., et al. 1999. Differential regulation of mammalian period genes and circadian rhythmicity by cryptochromes 1

and 2. *Proc. Natl. Acad. Sci.* **96:** 12114–12119.
von Gall, C., Duffield, G.E., Hastings, M.H., Kopp, M.D., Dehghani, F., Korf, H.W., and Stehle, J.H. 1998. CREB in the mouse SCN: A molecular interface coding the phase-adjusting stimuli light, glutamate, PACAP, and melatonin for clockwork access. *J. Neurosci.* **18:** 10389–10397.
Weinert, H., Weinert, D., Schurov, I., Maywood, E.S., and Hastings, M.H. 2001. Impaired expression of the mPer2 circadian clock gene in the suprachiasmatic nuclei of aging mice. *Chronobiol. Int.* **18:** 559–565.
Yagita, K., Yamaguchi, S., Tamanini, F., van der Horst, G.T., Hoeijmakers, J.H., Yasui, A., Loros, J.J., Dunlap, J.C., and Okamura, H. 2000. Dimerization and nuclear entry of mPER proteins in mammalian cells. *Genes & Dev.* **14:** 1353–1363.
Yagita, K., Tamanini, F., van der Horst, G.T.J., and Okamura, H. 2001. Molecular mechanism of the biological clock in cultured fibroblasts. *Science* **292:** 278–281.
Yagita, K., Tamanini, F., Yasuda, M., Hoeijmakers, J.H., van der Horst, G.T., and Okamura, H. 2002. Nucleocytoplasmic shuttling and mCRY-dependent inhibition of ubiquitylation of the mPER2 clock protein. *EMBO J.* **21:** 1301–1314.
Yamazaki, S., Numano, R., Abe, M., Hida, A., Takahashi, R., Ueda, M., Block, G.D., Sakaki, Y., Menaker, M., and Tei, H. 2000. Resetting central and peripheral circadian oscillators in transgenic rats. *Science* **288:** 682–685.
Yamazaki, S., Straume, M., Tei, H., Sakaki, Y., Menaker, M., and Block, G.D. 2002. Effects of aging on central and peripheral mammalian clocks. *Proc. Natl. Acad. Sci.* **99:** 10801–10806.
Yan, L. and Okamura, H. 2002. Gradients in the circadian expression of Per1 and Per2 genes in the rat suprachiasmatic nucleus. *Eur. J. Neurosci.* **15:** 1153–1162.
Yu, W., Nomura, M., and Ikeda, M. 2002. Interactivating feedback loops within the mammalian clock: BMAL1 is negatively autoregulated and upregulated by CRY1, CRY2, and PER2. *Biochem. Biophys. Res. Commun.* **290:** 933–941.
Zheng, B., Larkin, D.W., Albrecht, U., Sun, Z.S., Sage, M., Eichele, G., Lee, C.C., and Bradley, A. 1999. The mPer2 gene encodes a functional component of the mammalian circadian clock. *Nature* **400:** 169–173.
Zheng, B., Albrecht, U., Kaasik, K., Sage, M., Lu, W., Vaishnav, S., Li, Q., Sun, Z.S., Eichele, G., Bradley, A., et al. 2001. Nonredundant roles of the mPer1 and mPer2 genes in the mammalian circadian clock. *Cell* **105:** 683–694.
Zylka, M.J., Shearman, L.P., Weaver, D.R., and Reppert, S.M. 1998. Three period homologs in mammals: Differential light responses in the suprachiasmatic circadian clock and oscillating transcripts outside of brain. *Neuron* **20:** 1103–1110.